This article was downloaded by:
On: *14 January 2011*
Access details: *Access Details: Free Access*
Publisher *Taylor & Francis*
Informa Ltd Registered in England and Wales Registered Number: 1072954 Registered office: Mortimer House, 37-41 Mortimer Street, London W1T 3JH, UK

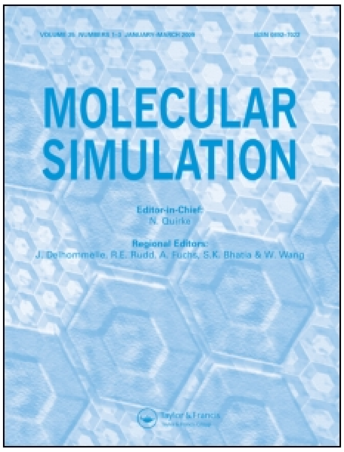

Molecular Simulation

Publication details, including instructions for authors and subscription information:
http://www.informaworld.com/smpp/title~content=t713644482

On the Relationship between Intramolecular Dynamics and the Density of States

Manel Canales[a]; Gemma Sesé †[a]
[a] Departament de Física i Enginyeria Nuclear, Universitat Politècnica de Catalunya, Barcelona, Spain

To cite this Article Canales, Manel and †, Gemma Sesé(2004) 'On the Relationship between Intramolecular Dynamics and the Density of States', Molecular Simulation, 30: 8, 529 — 535
To link to this Article: DOI: 10.1080/08927020410001680741
URL: http://dx.doi.org/10.1080/08927020410001680741

PLEASE SCROLL DOWN FOR ARTICLE

Full terms and conditions of use: http://www.informaworld.com/terms-and-conditions-of-access.pdf

This article may be used for research, teaching and private study purposes. Any substantial or systematic reproduction, re-distribution, re-selling, loan or sub-licensing, systematic supply or distribution in any form to anyone is expressly forbidden.

The publisher does not give any warranty express or implied or make any representation that the contents will be complete or accurate or up to date. The accuracy of any instructions, formulae and drug doses should be independently verified with primary sources. The publisher shall not be liable for any loss, actions, claims, proceedings, demand or costs or damages whatsoever or howsoever caused arising directly or indirectly in connection with or arising out of the use of this material.

Molecular Simulation, Vol. 30 (8), 15 July 2004, pp. 529–535

Taylor & Francis
Taylor & Francis Group

Downloaded At: 18:31 14 January 2011

On the Relationship between Intramolecular Dynamics and the Density of States

MANEL CANALES* and GEMMA SESÉ†

Departament de Física i Enginyeria Nuclear, Universitat Politècnica de Catalunya, Campus Nord-Mòdul B4, c/Jordi Girona 1-3, 08034 Barcelona, Spain

(Received February 2004; In final form February 2004)

The relationship between the intramolecular dynamics and the spectra has been analyzed by means of the molecular dynamics technique. Time autocorrelation functions of bond lengths, bending angles and torsional angles have been evaluated in a crystalline *trans*-polyacetylene system. The Fourier transforms of such functions have been compared with the densities of states obtained both for carbon and hydrogen atoms. This comparison is aimed at investigating the microscopic origin of the peaks which appear in the densities of states. This approach can be used in the analysis of the spectroscopic data of any molecular or polymeric system.

Keywords: Molecular dynamics simulation; Density of states; Time autocorrelation functions; Crystalline polymers

INTRODUCTION

Simulation has become a unique tool in the study of polymeric systems as it allows the comprehension at a microscopic level of a wide range of properties and phenomena taking place in these materials. Spectroscopy is one of the experimental techniques most widely used to characterize them. But the relation between spectral results and the microscopic features of the system is not direct. To ascertain the assignment of the bands to the microscopic dynamics of the sample, simulation techniques such as molecular dynamics (MD) can be very useful. The MD methodology has been extensively used in the study of polymers [1]. This technique allows the atomistic modeling of a material using only a knowledge of interatomic forces together with the assumption of classical mechanics [2]. MD is often used to mimic reality, but also to perform experiments which are not feasible, and to calculate functions which are not directly measurable.

Polyacetylene (PA) [3] is a crystalline polymer with linear chains. Atomistic simulation has already been employed in the calculation of a variety of its structural and dynamical properties [4–6]. The spectra of PA has been evaluated in MD simulations [7,8] resulting in a good agreement with the available experimental data [9–11]. In a previous work [8], the influence of microscopic interactions on the spectra has been studied by means of a series of MD imaginary experiments. The main goal of the present paper is to analyze the spectral results from a different point of view. A set of functions that are not directly measurable will be evaluated in a single MD simulation in order to get information about the microscopic origin of the features observed in experimental spectra. This approach can also be considered in the study of any system with intramolecular degrees of freedom.

In this work, we have performed a MD simulation of crystalline *trans*-PA. The considered force field has been previously tested and it satisfactorily reproduces the available experimental spectroscopic data [8]. Time autocorrelation functions of the intrachain degrees of freedom, i.e. skeletal bond lengths, bending angles and torsional angles, have been evaluated. Such functions are analyzed in the frequency domain and they are compared to the densities of states. This comparison allows the assignment of the main spectral peaks to the dynamics of specific intramolecular quantities.

---

*Corresponding author. E-mail: manel.canales@upc.es
†E-mail: gemma.sese@upc.es

ISSN 0892-7022 print/ISSN 1029-0435 online © 2004 Taylor & Francis Ltd
DOI: 10.1080/08927020410001680741

Additional information on the microscopic dynamics of the system will also be presented.

The paper is organized as follows. Simulation details are summarized in the second section. Simulation results are presented in the third section. The results of this work are discussed in the fourth section. Some concluding remarks are gathered in the final section.

SIMULATION DETAILS

Crystalline *trans*-PA ($(CH)_n$) has been simulated. Carbon and hydrogen atoms have been explicitly taken into account. The considered force field includes (1) stretching, (2) bending, (3) torsional and (4) non-bonded interactions. The C—H bond lengths have been constrained to the equilibrium values by means of the SHAKE algorithm [12]. Stretching forces between carbon atoms have been calculated and alternating double and single bonds have been considered. Two different sets of bending parameters have been used depending on whether or not hydrogen atoms are involved. As for the torsional forces, two sets of parameters have been used depending on whether the central CC bond is single or double. Non-bonded interactions are included between atoms located in different chains and between those within the same chain provided that they are separated by three or more bonds. If they are separated exactly by three bonds, half of the calculated force has been taken into account. The aforementioned interactions are given by

$$V^{\mathrm{ST}}(r) = \frac{1}{2}k^{\mathrm{ST}}(r - r_0)^2, \tag{1}$$

$$V^{B}(\theta) = \frac{1}{2}k^{B}(\theta - \theta_0)^2, \tag{2}$$

$$V^{\mathrm{TO}}(\phi) = \frac{1}{2}k^{\mathrm{TO}}(\phi - \phi_0)^2, \tag{3}$$

$$V^{\mathrm{NB}}(r) = \sum_{i}^{N}\sum_{l}^{N}\left(A\exp\left(\frac{-r}{\rho}\right) - \frac{B}{r^6}\right), \tag{4}$$

where r is the distance between atoms, θ is the bending angle and ϕ is the dihedral angle, and r_0, θ_0 and ϕ_0 are their equilibrium values. The corresponding potential parameters are collected in Table I. These potentials are the same as those considered in our previous work [8], where a general good agreement was obtained between the available neutron scattering measurements and the densities of states of hydrogen atoms. At this point it is interesting to note that the neutron spectroscopic results are dominated by the signal coming from hydrogen atoms. Nevertheless, the densities of states of carbon atoms should display peaks at the same frequencies because of the rigidity of the C—H bonds.

TABLE I Parameters for the stretching, bending, torsional and non-bonded potentials used in the simulation

Interaction	*Parameters*		
C—C	$k_1^{\mathrm{ST}} = 11.5$	$r_{01} = 1.446$	
C=C	$k_2^{\mathrm{ST}} = 13.0$	$r_{02} = 1.346$	
CCC	$k_1^{B} = 5.5$	$\theta_{01} = 125.5°$	
CCH	$k_2^{B} = 3.1$	$\theta_{02} = 117.35°$	
···C—C···	$k_1^{\mathrm{TO}} = 0.05$	$\phi_{01} = 180°$	
···C=C···	$k_2^{\mathrm{TO}} = 0.75$	$\phi_{02} = 180°$	
C···C	$A_1 = 3627.4$	$\rho_1 = 0.2778$	$B_1 = 24.64$
C···H	$A_2 = 380.22$	$\rho_2 = 0.2725$	$B_2 = 5.422$
H···H	$A_3 = 115.12$	$\rho_3 = 0.2624$	$B_3 = 1.184$

Distances are given in Å, energies in eV and angles in degrees.

The densities of states parallel ($C_{\parallel}(\omega)$) and perpendicular ($C_T(\omega)$) to the chain axis have been evaluated for both hydrogen and carbon atoms. They are defined as

$$C_{\parallel}(\omega) = \int_0^{\infty} < v_{\parallel}(t)v_{\parallel}(0) > \sin(\omega t)\,\mathrm{d}t, \tag{5}$$

$$C_T(\omega) = \int_0^{\infty} < v_T(t)v_T(0) > \sin(\omega t)\,\mathrm{d}t, \tag{6}$$

where $v_{\parallel}$ is the component of the atomic velocity parallel to the chain axis (z direction) and v_T refers to a component of the velocity perpendicular to the chain axis. $C_T(\omega)$ has been obtained by averaging over directions x and y.

A crystalline structure with planar chains, whose unit cell is referred as the *out-of-phase* structure [13], is taken as the initial configuration of the simulation. The simulated sample consists of 16 chains, each of them comprising 128 (—CH—) units. There are 4096 atoms in the simulation box whose dimensions are 14.64, 16.96 and 158.72 Å in the x, y and z directions, respectively. The axes of all the chains are parallel to the z axis and the angle between the plane of a chain and the x axis has been set to 22°. The chains have been located in a cubic box with periodic boundary conditions. A cut-off of half the size of the cubic cell in the x direction was used to compute the non-bonded interactions. The integration of the equations of motion has been performed by means of the leap-frog Verlet algorithm, with a time step of 1 fs. Production runs of 100 ps have been performed in the (N, V, T) ensemble [14] at 298 K after equilibration runs of 2 ps.

RESULTS

Stretching

We begin our consideration of the intrachain dynamics by examining stretching motion between

Downloaded At: 18:31 14 January 2011

Downloaded At: 18:31 14 January 2011

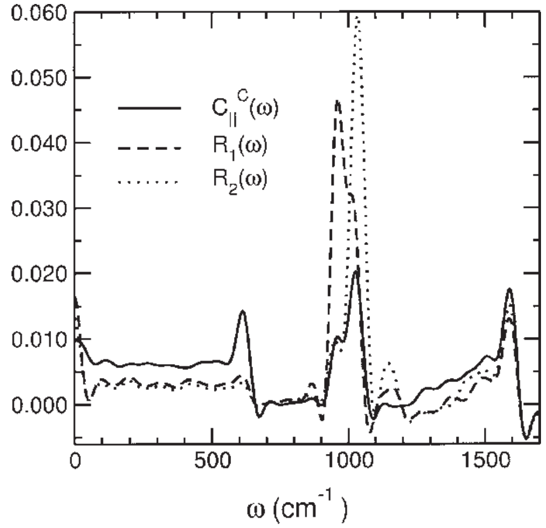

FIGURE 1 Density of states in the direction parallel to the chain axis ($C_{||}(\omega)$) for carbon atoms, and Fourier transforms of the autocorrelation functions of bond lengths corresponding to single ($R_1(\omega)$) and double ($R_2(\omega)$) CC bonds.

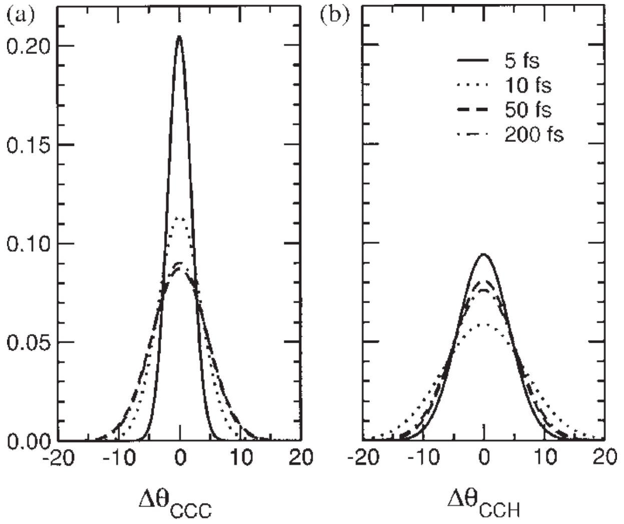

FIGURE 2 Distribution probabilities of an angular change $|\Delta\theta|$ for the CCC (a) and CCH (b) bending angles during several time intervals.

carbon atoms The autocorrelation function of the bond lengths has been obtained by the following

$$R_k(t) = \frac{\langle (r(t) - r_0)(r(0) - r_0) \rangle}{\langle (r(0) - r_0)^2 \rangle}, \qquad (7)$$

where k stands for 1 or 2 depending on whether the bond is single or double. These functions are obtained after averaging over all bonds in the system, and over several time origins. In order to analyze these functions in the frequency domain, their Fourier transforms, namely $R_1(\omega)$ and $R_2(\omega)$, have been evaluated. They are displayed in Fig. 1. The most relevant peak in $R_1(\omega)$ takes place at about 950 cm^{-1} and the one in $R_2(\omega)$ at about 1040 cm^{-1}. Both functions display a secondary peak at about 1590 cm^{-1}. Peaks at all these frequencies are observed in the $C_{||}(\omega)$ for carbon atoms, which is also shown in Fig. 1. This function shows important peaks at 625, 1040 and 1590 cm^{-1}, and a shoulder at about 950 cm^{-1}. Even though there is no experimental information about this function, some of these frequencies will be found in the $C_{||}(\omega)$ for hydrogen atoms because of the C—H constraint.

Bending

We have also analyzed the dynamics of bending angles. Figure 2a,b shows the probability of an angular change $|\Delta\theta| = |\theta - \theta_0|$ for CCC and CCH bending angles, respectively, during various time intervals. This probability is normalized to unity. The equilibrium distribution of CCH angles is slightly wider than the one of the CCC angles, which is consistent with the fact that $k_{CCC} > k_{CCH}$. Some discrepancies are apparent for the short time dynamics. First, when very short time intervals are considered, the range of variability is smaller for CCC angles than for CCH angles. In addition, the equilibrium distribution is reached faster for CCC than for CCH angles.

The autocorrelation functions of CCC and CCH bending angles, $B_1(t)$ and $B_2(t)$, respectively, have also been obtained by the following

$$B_l(t) = \frac{\langle (\theta(t) - \theta_0)(\theta(0) - \theta_0) \rangle}{\langle (\theta(0) - \theta_0)^2 \rangle}. \qquad (8)$$

No significant differences have been detected between the functions corresponding to C—C—H and C═C—H as only one CCH bending potential has been considered. Then, $B_2(t)$ has been evaluated by averaging over both types of bending angles. The Fourier transforms of Eq. (8), $B_1(\omega)$ and $B_2(\omega)$, have been evaluated. They are shown in Fig. 3 together with the $C_{||}(\omega)$ for hydrogen atoms. The three functions display a peak at 625 cm^{-1}, which is much more important in $B_1(\omega)$. Two secondary peaks also appear in $B_1(\omega)$ at about 985 and 1160 cm^{-1}. As for $B_2(\omega)$, it displays very relevant peaks at 1015 and 1285 cm^{-1}, and a secondary one at 1590 cm^{-1}. Relevant peaks appear in $C_{||}(\omega)$ for hydrogen atoms at 1015 and 1285 cm^{-1}, together with secondary peaks at 625 and 1590 cm^{-1}.

Torsion

Two different sets of parameters for the torsional potential (3) have been considered in our simulation, depending on whether the central bond of the dihedral angle is single or double.

The probability distributions of an angular change $|\Delta\phi| = |\phi - \phi_0|$ for the CC—CC, CC—CH and HC—CH dihedrals have been calculated during various time intervals. These functions are shown in

Fig. 4. When time intervals of few time steps are considered, the range over which CC—CC angles have changed is the smallest and the one for HC—CH is the largest (Fig. 4a). The range over which all of them have changed increases with the length of the considered time interval, but there are no significant differences between them for larger time intervals. For periods larger than 50 fs, the probability distributions for all these dihedrals do not show important changes and deviation from their initial values is always lower than 50° (Fig. 4b).

The autocorrelation functions of CC—CC, CC—CH and HC—CH dihedral angles, $T_{10}(t)$, $T_{11}(t)$ and $T_{12}(t)$, respectively, have also been obtained by the following

$$T_{1l}(t) = \frac{\langle (\phi(t) - \phi_0)(\phi(0) - \phi_0) \rangle}{\langle (\phi(0) - \phi_0)^2 \rangle}. \tag{9}$$

Their Fourier transforms $T_{10}(\omega)$, $T_{11}(\omega)$ and $T_{12}(\omega)$ have been evaluated. They are shown

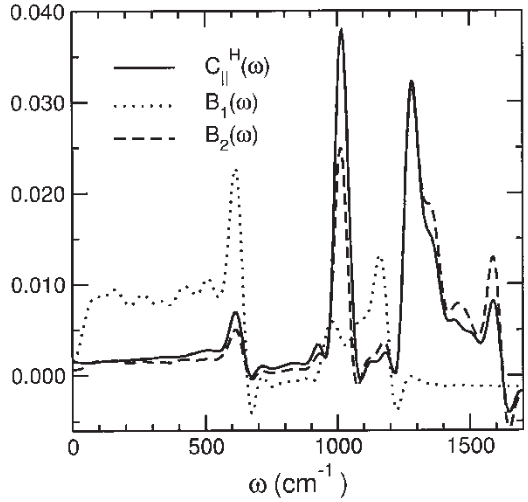

FIGURE 3 Density of states in the direction parallel to the chain axis ($C_{\parallel}(\omega)$) for hydrogen atoms, and Fourier transforms of the autocorrelation functions of bending angles corresponding to the CCC ($B_1(\omega)$) and CCH ($B_2(\omega)$) angles.

Downloaded At: 18:31 14 January 2011

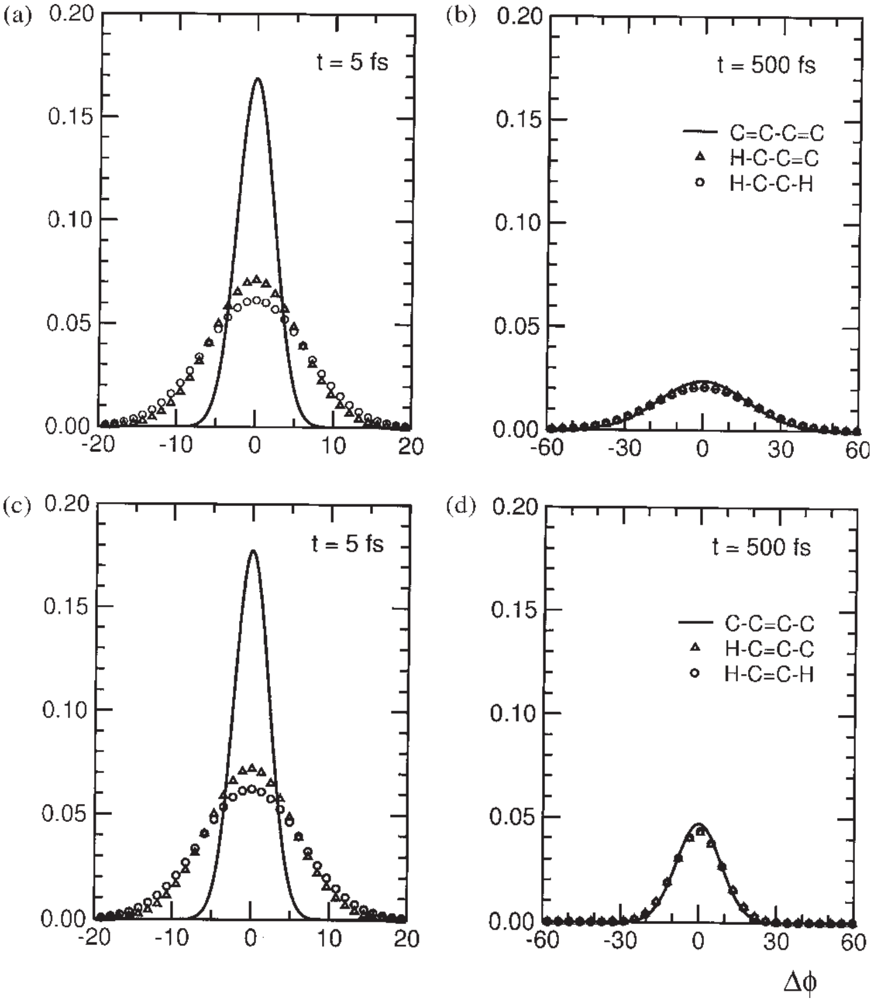

FIGURE 4 Distribution probabilities of an angular change $|\Delta\phi|$ for the $\cdots$C—C$\cdots$ ((a) and (b)) and $\cdots$C═C$\cdots$ ((c) and (d)) dihedral angles during several time intervals.

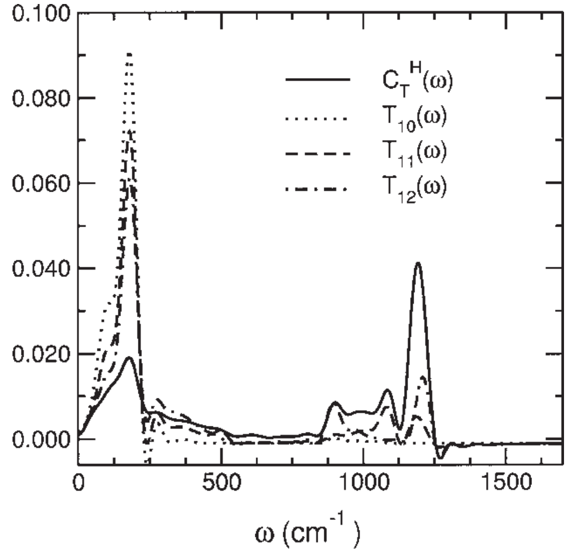

FIGURE 5 Density of states in the direction perpendicular to the chain axis ($C_T(\omega)$) for hydrogen atoms, and Fourier transforms of the autocorrelation functions of dihedral angles corresponding to the CC—CC ($T_{10}(\omega)$), HC—CC ($T_{11}(\omega)$) and HC—CH ($T_{12}(\omega)$) angles.

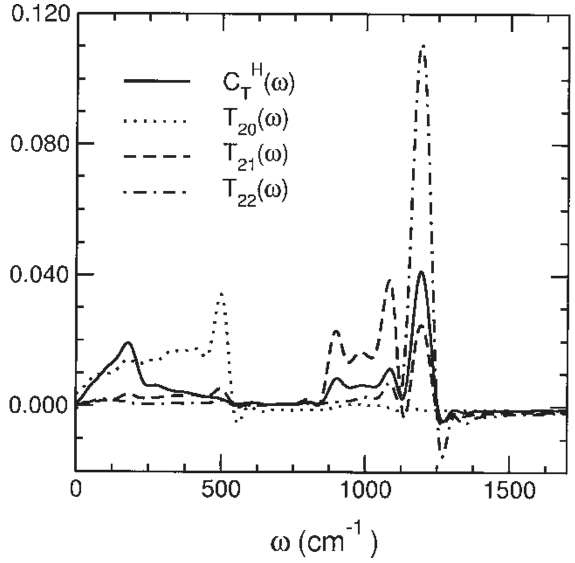

FIGURE 6 Density of states in the direction perpendicular to the chain axis ($C_T(\omega)$) for hydrogen atoms, and Fourier transforms of the autocorrelation functions of dihedral angles corresponding to the CC=CC ($T_{20}(\omega)$), HC=CC ($T_{21}(\omega)$) and HC=CH ($T_{22}(\omega)$) angles.

Downloaded At: 18:31 14 January 2011

in Fig. 5 together with the $C_T(\omega)$ for hydrogen atoms because it has been shown [8] that torsional forces do specially influence the density of states perpendicular to the chain axis. Only one peak is remarkable in $T_{10}(\omega)$ at about $175\,\mathrm{cm}^{-1}$, with a shoulder at about $100\,\mathrm{cm}^{-1}$. Both the peak and the shoulder also appear in $T_{11}(\omega)$ and $T_{12}(\omega)$. Then the dynamics of all the ···C—C··· dihedrals take place, at least, at this frequency, especially the CC—CC one, because of the relative relevance of the corresponding peak. In the $T_{11}(\omega)$, two much smaller peaks appear at about 1090 and $1190\,\mathrm{cm}^{-1}$. Two secondary peaks are apparent in $T_{12}(\omega)$ at about 900 and $1190\,\mathrm{cm}^{-1}$. All these peaks also appear in the $C_T(\omega)$ for hydrogen atoms.

As for the dynamics of the dihedrals having a double central bond, the probability of an angular change $|\Delta\phi|$ for the CC=CC, CC=CH and HC=CH dihedrals during various time intervals have also been evaluated. They are shown in Fig. 4c,d. The dependence of $|\Delta\phi|$ on the considered time interval is qualitatively the same as the one observed for the dihedrals having a single central bond. That is, for short time intervals it depends very much on the type of atoms involved, and for large time intervals it basically depends on the potential force constant. The equilibrium distribution is reached after 20 fs for the CC=CC angles, after 100 fs for the CC=CH angles and after 500 fs for the HC=CH angles, being the deviations from their corresponding ϕ_0 values always smaller than for the ···C—C··· dihedrals. And there are no differences between the equilibrium distributions of all the ···C=C··· dihedrals.

The autocorrelation functions of CC=CC, CC=CH and HC=CH angles, $T_{20}(t)$, $T_{21}(t)$ and $T_{22}(t)$, respectively, have been evaluated analogously to Eq. (9). Their Fourier transforms $T_{20}(\omega)$, $T_{21}(\omega)$ and $T_{22}(\omega)$ are shown in Fig. 6. For comparison, $C_T(\omega)$ for hydrogen atoms is also shown. Only one peak is relevant in $T_{20}(\omega)$ at about $500\,\mathrm{cm}^{-1}$, which is preceded by a wide band between 100 and $450\,\mathrm{cm}^{-1}$. Three peaks appear in $T_{21}(\omega)$ at about 900, 1090 and $1190\,\mathrm{cm}^{-1}$. $T_{22}(\omega)$ displays only one very important peak at about $1190\,\mathrm{cm}^{-1}$.

DISCUSSION

The dynamics of bending and torsional angles take place on short time scales. Rapid motions establish an equilibrium distribution within the corresponding potential well. For very short time intervals, the probability distributions for both bending and torsional angles depend very much on the type of atoms. In particular, they are wider when hydrogen atoms are explicitly involved. When longer time intervals are considered, these functions depend on the particular value of the potential force constant. Then, the differences between CCC and CCH bending angles distributions are negligible, and the ···C=C··· distributions are markedly stiffer than those for the ···C—C··· dihedrals. As for their equilibrium distributions, they are reached faster for the skeletal angles, which explicitly involve carbon

Downloaded At: 18:31 14 January 2011

atoms only. The bending and dihedral equilibrium distributions are obtained after 200 and 500 fs, respectively.

The bands observed in the densities of states for both carbon and hydrogen atoms are also present in one or more correlation functions that characterize stretching, bending and torsional motions defined by Eqs. (7), (8) and (9), respectively. Table II contains a summary of the main peaks observed in the densities of states and of the interactions which are most likely responsible for them, according to our results. They are in good agreement with the ones obtained in our previous work [8].

As the CH bond is constrained, the dynamics of hydrogen atoms, which can be more directly related to experiment, is strongly influenced by the most relevant frequencies characterizing the dynamics of carbon atoms. The $C_{\|}(\omega)$ for carbon atoms displays two main peaks at 625 and 1590 cm^{-1}, a secondary one at 1040 cm^{-1}, and a shoulder at 950 cm^{-1}. As there is an important peak at 625 cm^{-1} in $B_1(\omega)$, CCC bending originates such peak. $R_1(\omega)$ and $R_2(\omega)$ display relevant peaks at about 1590 cm^{-1}. Then, stretching between carbon atoms is mainly responsible for it. It is probably influenced by the CCH bending because a peak at this frequency is observed in $B_2(\omega)$. As for the secondary peak at 1040 cm^{-1}, both CC stretching and CCC bending contribute to it because $R_1(\omega)$, $R_2(\omega)$ and $B_1(\omega)$ do show peaks at frequencies close to this one. But we think that the most important contribution comes from the CCH bending because $B_2(\omega)$ displays a remarkable peak at 1015 cm^{-1}. Besides, the peak observed at about this frequency is much more relevant in $C_{\|}(\omega)$ for hydrogen atoms than in $C_{\|}(\omega)$ for carbon atoms.

The $C_{\|}(\omega)$ for hydrogen atoms displays two very important peaks at 1015 and 1285 cm^{-1}. Analogous peaks at the same frequencies can be found in $B_2(\omega)$, which means that CCH bending is mainly responsible for them. As stated in the previous paragraph, CCC bending and CC stretching also contribute to the one at 1015 cm^{-1}, but in a lower degree. As for the two much smaller peaks at 625 and at 1590 cm^{-1}, we believe that they appear in $C_{\|}(\omega)$ for hydrogen atoms because of the geometrical constrain between carbon and hydrogen atoms, but they are more relevant for the carbon dynamics.

TABLE II Main peaks observed in the densities of states defined by Eqs. (5) and (6) and most likely interactions responsible for them

$C_{\|}(\omega)$ *for H*	$C_{\|}(\omega)$ *for C*	$C_T(\omega)$ *for H*	*Interaction*
		175	CC—CC torsion
625	625		CCC bending
		900	HC═CC torsion (HC—CH torsion)
1015	960–1030		CCH bending (CC stretching–CCC bending)
		1090	HC═CC torsion (HC—CC torsion)
		1190	HC═CH torsion
1285			CCH bending
1590	1590		CC stretching (CCH bending)

When two interactions are given, the less relevant contribution is quoted in brackets. Frequencies are given in cm^{-1}.

All the relevant peaks appearing in the $C_T(\omega)$ for hydrogen atoms have been observed in the Fourier transforms of the correlation functions of torsion angles. As shown in Fig. 5, $C_T(\omega)$ displays two important peaks at about 175 and 1190 cm^{-1}, and a band with two relative maxima at 900 and 1090 cm^{-1}. From the relative relevance of every peak, it is possible to relate their frequencies to the dynamics of specific dihedrals. Even though the dynamics of all $\cdots$C—C$\cdots$ dihedrals contribute to the peak at 175 cm^{-1}, the CC—CC one seems to be more relevant. The dynamics of HC—CH angles contributes mainly to the peaks at 900 and 1190 cm^{-1}, and the HC—CC one to the peaks at 1090 and 1190 cm^{-1}. Whereas CC═CC torsions are mainly characterized by frequencies lower than 500 cm^{-1}, the dynamics of HC═CC and HC═CH dihedrals takes place mainly at frequencies around 1000 cm^{-1}, as shown in Fig. 6. Because of the relative relevance of the peaks observed in $T_{21}(\omega)$ and $T_{22}(\omega)$, the HC═CH dynamics is responsible for the peak at 1190 cm^{-1} and so is the HC═CC dynamics for the 900 and 1090 cm^{-1} peaks.

CONCLUDING REMARKS

The dynamics of bending and torsional angles has been analyzed in a MD simulation of *trans*-PA. It has been shown that for very short time intervals, the distributions of both bending and dihedral angles are wider when hydrogen atoms are involved. For larger time intervals, smaller than 200 and 500 fs for bending and dihedral angles, respectively, the equilibrium distributions are reached. They basically depend on the corresponding force constant.

We have presented a methodology which can be used to analyze the vibrational spectra of any molecular system. Time correlation functions of bond lengths, bond angles and torsion angles have been evaluated. The analysis of such functions has proved to be very useful in order to investigate the microscopic origin of the peaks obtained in the densities of states. It has been shown that the dynamics of every intrachain degree of freedom under study is characterized by one or more frequencies which have also been observed in the densities of states.

Acknowledgements

Financial support of DGICYT (Project BFM2000-0596-C03-02) and of Generalitat de Catalunya (Project 2001SGR 00222) is acknowledged.

References

[1] Binder, K. (1995) *Monte Carlo and Molecular Dynamics Simulations in Polymer Science* (Oxford University Press, New York).

[2] Allen, M.P. and Tildesley, D.J. (1987) *Computer Simulation of Liquids* (Clarendon Press, Oxford).

[3] Chien, J.C.W. (1984) *Polyacetylene: Chemistry, Physics and Material Science* (Academic Press, New York).

[4] Corish, J., Hanratty, V.C.A., Morton-Blake, D.A., Benière, F. and Morin, A. (1990) "Atomistic simulation calculations on the structures of conducting polymers: Part I. Pristine polyacetylene and polyparaphenylene", *J. Mol. Struct.* **207**, 41.

[5] Sesé, G. and Catlow, C.R.A. (1993) "A molecular dynamics study on pristine and doped polyacetylene", *Phil. Mag. B* **68**, 397.

[6] Papanek, P. and Fischer, J.E. (1993) "Molecular-dynamics simulation of crystalline *trans*-polyacetylene", *Phys. Rev. B* **48**, 12566.

[7] Dianoux, A.J., Kneller, G.R., Sauvajol, J.L. and Smith, J.C. (1993) "The polarized density of states of crystalline polyacetylene. Molecular dynamics analysis and comparison with neutron scattering results", *J. Chem. Phys.* **99**, 5586.

[8] Canales, M. and Sesé, G. (2003) "Influence of microscopic interactions on the spectra of polyacetylene", *J. Chem. Phys.* **118**, 4237.

[9] Maconnachie, A., Dianoux, A.J., Shirakawa, H. and Tasumi, M. (1986) "Incoherent inelastic neutron scattering from polyacetylenes in the 3500–400 cm^{-1} region", *Synth. Met.* **14**, 323.

[10] Sauvajol, J.L., Djurado, D., Dianoux, A.J., Theophilou, N. and Fischer, J.E. (1991) "Polarized vibrational density of states of polyacetylene from incoherent inelastic neutron scattering", *Phys. Rev. B* **43**, 14305.

[11] Hirata, S., Torii, H., Furukawa, Y., Tasumi, M. and Tomkinson, J. (1996) "Inelastic neutron scattering from *trans*-polyacetylene", *Chem. Phys. Lett.* **261**, 241.

[12] Ryckaert, J.P., Cicotti, G. and Berendsen, H.J.C. (1977) "Numerical integration of the Cartesian equations of motion of a system with constraints: molecular dynamics of *n*-alkanes", *J. Comp. Phys.* **23**, 327.

[13] Chien, J.C.W., Karasz, F.E. and Shimamura, K. (1982) "An estimate of bond length alteration in *trans*-PA", *Makromol. Chem. Rapid Commun.* **3**, 655.

[14] Berendsen, H.J.C., Postma, J.P.M., Van Gunsteren, W.F., DiNola, A. and Haak, J.R. (1984) "Molecular dynamics with coupling to an external bath", *J. Chem. Phys.* **81**, 3684.

Downloaded At: 18:31 14 January 2011